Dalton Transactions

Accepted Manuscript

ROYAL SOCIETY OF CHEMISTRY

www.rsc.org/dalton

Journal Name

ARTICLE

Group 13 metal complexes containing the bis-(4-methyl-benzoxazol-2-yl)-methanide ligand†‡

Received 00th January 20xx,
Accepted 00th January 20xx

DOI: 10.1039/x0xx00000x

www.rsc.org/

David-R. Dauer, Melchior Flügge, Regine Herbst-Irmer, Dietmar Stalke*[a]

To focus on the high importance of low-valent main group metal complexes, which can be applied to catatyic transformations, this article deals with the promising new ligand system (4-Me-$NCOC_6H_3)_2CH_2$ (**1**). It is patterned on the well known nacnac ligand and a further development of the parent bisheterocyclo methanes. In comparison to the results of previous works based on the bisheterocyclo methanes $(NCOC_6H_4)_2CH_2$ and $(NCOC_6H_4)_2CH_2$ derivative **1** was modified by adding a methyl group to the annulated benzene perimeters to enhance the steric protection of a potentially coordinated main group metal cation. Upon reaction of **1** with group 13 trimethyl reagents and dialkyl aluminium halides the ligand backbone gets deprotonated and the two endocyclic nitrogen donor atoms coordinate the remaining organometallic fragment to form a six-membered metalla heterocycle. The synthesis of [Me_2Al{(4-Me-$NCOC_6H_3)_2CH$}] (**2**), [Me_2Ga{(4-Me-$NCOC_6H_3)_2CH$}] (**3**), [Me_2In{(4-Me-$NCOC_6H_3)_2CH$}] (**4**), [ClMeAl{(4-Me-$NCOC_6H_3)_2CH$}] (**5**), [IMeAl{(4-Me-$NCOC_6H_3)_2CH$}] (**6**) and [IEtAl{(4-Me-$NCOC_6H_3)_2CH$}] (**7**) could be accomplished. A structural comparison of those metallated species based on single crystal X-ray analyses identifies them as ideal precursors generating new low-valent main group complexes.

Introduction

In the context of the ongoing increasing demand in the activation of small molecules like H_2, N_2, NH_3 or CO_2 the development of new synthetic approaches for generating catalytic active species is of high interest. Even though this research area of catalytic activation is mostly focussed on the field of transition metal complexes the transfer to suitable main group metal complexes, which should adopt the same catalytic reactivity compared to the transition metals or even exceed them, plays a key role in current research.[1]

As figurehead for efficient small molecule activation the FLP chemistry (frustrated Lewis pairs) developed to a promising research area over the last decade.[2] In this course the usage of mainly phosphorus/boron, nitrogen/boron or carbon/boron FLP systems offers a simple access to the efficient splitting of dihydrogen[3] or ring opening of THF.[4] Also the aluminium based FLP's were found to be advantageous for B-H or N-H bond activation[5], polymerisation reactions of methyl methacrylate[6] and conversion of CO_2.[7] Furthermore, the well-known nacnac ligand and the derived main group metal complexes, respectively, facilitate the stabilisation of metal ions in low oxidation states.[8] The synthesis of the first Mg(I) compound[9] and corresponding β-diketiminate Ca(II) complexes,[10] which were successfully applied for epoxide/CO_2 copolymerisation[11] or hydrogenation reactions of alkenes with H_2,[12] should be highlighted as alkaline earth metal complexes performing in catalysis. Switching to group 13 elements also a variety of Al(III) and Ga(III) containing complexes was synthesised and fully characterized.[13] Subsequently also the low-valent Al(I)[14] and Ga(I)[15] species employing the Dipp-substituted (Dipp = 2,6-diisopropylphenyl) nacnac ligand were accessible. More recently the catalytic activity of the related alumoxanes was studied in detail.[16] Other common ligand types, which are used for stabilisation of dimeric low-valent group 13 species involving metal-metal multiple bonds, are the substituted terphenyls, which are also prone for interaction with small molecules like H_2.[17]

With this in mind in the field of main group transformations ligand design in particular and the choice of the suitable main group element has a significant influence on the stability and the catalytic abilities of the resulting compounds. In this work we tried to mimick the omnipresent nacnac ligand by two methylene bridged substituted benzoxazole moieties. The corresponding group 13 metal complexes were synthesised to get the best from two words: the stabilisation abilities to get low-valent metal complexes and the reactivity of group 13 metals. To tie up to earlier studies concerning related bisheterocyclo methanide[18] and amide derivatives[19] this work focuses on bis-(4-methylbenzoxazol-2-yl)-methane **1**. The previous results of the methanide containing metal complexes have shown that upon deprotonation of the methylene bridge of the parent ligand systems the coordination of the metal cation is preferentially accomplished by the endocyclic

[a] *Institut für Anorganische Chemie, Georg-August-Universität Göttingen, Tammannstraße 4, 37077 Göttingen, Germany*
E-mail: dstalke@chemie.uni-goettingen.de.

† Dedicated to Prof. Herbert W. Roesky on the occasion of his 80th birthday.

‡Electronic Supplementary Information (ESI) available: Tables of data collection parameters, bond lengths and angles of compounds **1** – **7** and further information for side product **1a**. For ESI and crystallographic data in CIF or other electronic format see DOI: 10.1039/x0xx00000x

nitrogen donor atoms in a chelating fashion.[20] Due to this fact and to further shield the coordinated metal the bis-(benzoxazol-2-yl)-methane ligand was additionally methyl substituted in **1** to increase the kinetic stabilisation at the same side of the coordinating nitrogen atoms. Neither in the case of the methanide nor the amide derivatives a coordination via the other feasible O- or S-coordinating sites was observed in the solid state yet.[19, 18]

The issue of steric shielding of metal centres within the group 13 complexes is an important aspect for the further applications and reactions, because in the future we plan to convert these Al(III) containing species to the low-valent Al(I) compounds like e. g. [Al{Dipp$_2$nacnac}].[14e] Because of the high electrophilicity of the Al(I) species steric protection is essential to maintain the monomeric carbene-like structural motif and prevent dimerisation or nucleophilic attacks.[21] The challenge to synthesise a low-valent species containing a bisheterocyclo methanide ligand backbone is still the guiding idea of ongoing research and **1** seems to be a promising ligand system for subsequent reduction steps (*vide infra*).

Among the nacnac derivatives and the bisheterocyclo methanides the efficient metal shielding is within some limits comparable. In the case of the nacnac ligands the residues at the bulky imine moieties are twisted nearly perpendicular with respect to the chelating C_3N_2M-plane, which causes the metal atoms to be most protected. In the case of the complexes derived from **1** the methyl groups shield as well but due to less steric congestion the metal centres are slightly more accessible to allow some specific substitution reactions. The new metal complexes containing a central six-membered metalla heterocycle are reminiscent to the analogue metal complexes with the omnipresent nacnac ligand. Following similarities between the herein discussed bisheterocyclo methanides and the nacnac ligands can be stated due to the structural comparison of the corresponding metal complexes: At first the deprotonation of the bridging moiety leads to the formation of a negative charge in the ligand's backbone, which is completely delocalised to give a 6π electrons containing metalla heterocycle (see Table 1). Secondly, the chelating coordination of the metal cation is achieved exclusively by the two nitrogen donor atoms in the ligand periphery.

Results and Discussion

Ligand synthesis:

The synthesis of the parent uncharged ligand system is achieved as reported earlier for the corresponding unsubstituted bis-(benzoxazol-2-yl)- and bis-(benzothiazol-2-yl)-methanes.[18, 22] A cyclocondensation reaction of two equivalents of 2-amino-3-methylphenol and one equivalent of a C_3-linker unit derived from malonic acid yields the ligand. Two different synthesis routes were performed and optimised to give a moderate overall yield of 56 % (see Scheme 1).

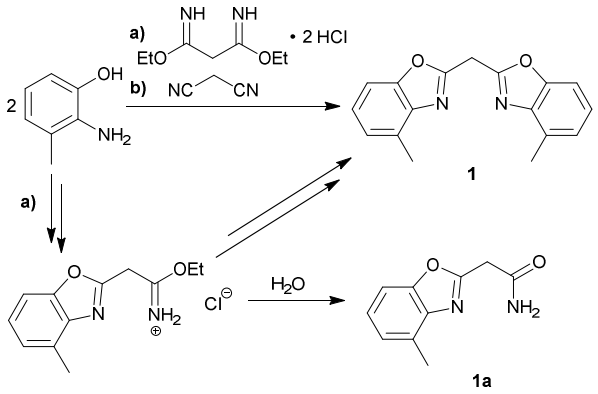

Scheme 1. Synthetic routes to the parent ligand system **1** including the side product **1a**.

The first route is along the synthesis of the unsubstituted bis-(benzoxazol-2-yl)-methane, in which a bisimidate linker was used for the coupling of the two phenol derivatives. This pathway, however, leads to a smaller yield of the desired product **1** and also promotes the formation of a specific side product **1a**. The side product could be identified as 4-methylbenzoxazol-2-yl-carboxamide, which occurs, if just one equivalent of the starting material has cyclised and the remaining imidate unit has been hydrolysed upon further purification. On the second improved route malonic dinitrile was added to the phenolic starting material. In that case polyphosphoric acid (ppa) was added as solvent and catalytically facilitates the cyclisation reaction to give the parent ligand system **1**.

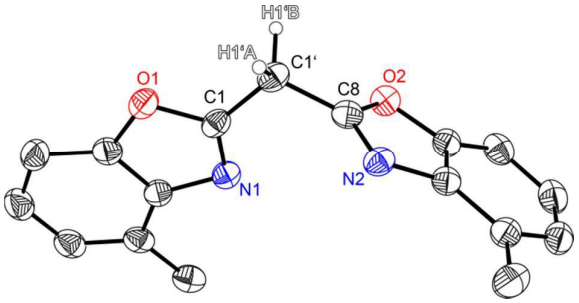

Figure 1. Molecular structure of (4-Me-NCOC$_6$H$_3$)$_2$CH$_2$ (**1**). Anisotropic displacement parameters are depicted at the 50 % probability level. C-H hydrogen atoms are omitted for clarity except the bridging ones. Structural data are given in Tables 1 – 3.

Compound **1** crystallises in the triclinic space group $P\bar{1}$ and the asymmetric unit contains one molecule. Like the other symmetrically substituted bisheterocyclo methanes[18] the central carbon atom C1' is also coordinated in a distorted tetrahedral fashion and the benzoxazol moieties are twisted nearly perpendicular (81.53(4) °) relative to each other. Due to the higher steric demand of the heterocycles the C1-C1'-C8 angle is widened to 110.8(1) °, whereas all other angles around C1' are slightly compressed in comparison to an ideal tetrahedral angle. Interestingly in the solid state **1** forms a 3D network of quite remarkable C-H···N hydrogen bonds, in which the two acidic methylene hydrogen atoms of the bridge are coordinated by imine nitrogen atoms of two adjacent

molecules (see Figure 2). The experimentally determined values show two hydrogen bonds each, which are energetically more favourable (H1'B···N2: 2.39 Å; C1'-H1'B···N2: 171.1 °), and two which are less pronounced (H1'A···N1: 2.62 Å; C1'-H1'A···N1: 150.9 °).

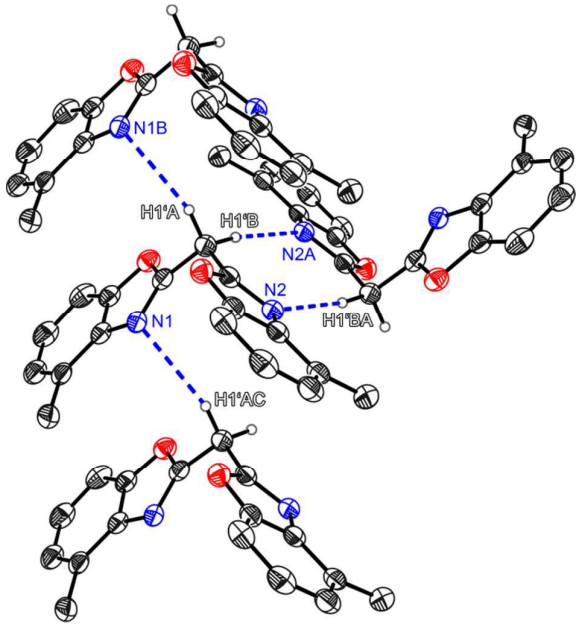

Figure 2. Hydrogen bonding properties of the parent ligand system (4-Me-$NCOC_6H_3)_2CH_2$ (**1**).

Syntheses of the group 13 metal complexes:

The reaction of **1** in toluene with pure trimethyl aluminium, gallium or indium lead to the formation of the monoanionic methanides containing the corresponding MMe_2 fragment (see Scheme 2). By addition of these organometallic reagents the acidic methylene bridge gets deprotonated under evolution of gaseous methane and in a concerted manner the remaining dimethyl group 13 metal cation gets chelated by the two ring nitrogen donor atoms.

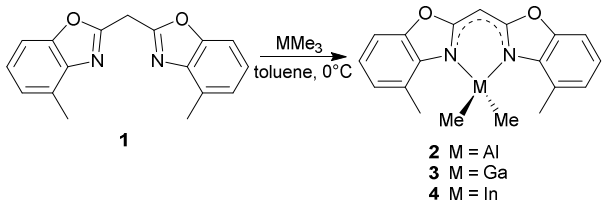

Scheme 2. Metallation reactions of **1**.

Upon deprotonation the concerning C_{ipso}-C_{bridge} distances are shortened in comparison to **1** and the C_{ipso}-N distances are slightly elongated (Table 1). This is caused by two facts, which are important for the structural features. On the one hand the deprotonation of the central methylene moiety generates a free electron pair. Because of the adjacent conjugated π-systems of the two benzoxazole units this free electron pair tends to be delocalised over the whole ligand framework resulting in different feasible resonance structures: carb-anionic, amidic or completely delocalised. On the other hand the hybridisation of the central carbon atom changes from sp^3 in the starting material **1** to sp^2 in the metallated species **2 – 4** based on the trigonal planar coordination geometry of C1'.

Structural comparison of 2 – 4:

A closer look at the experimentally determined geometry of **1** shows that the C_{ipso}-C_{bridge} distance is slightly shorter than it is to be expected for a typical C(sp^2)-C(sp^3) single bond (1.51 Å). This deviation can be explained by the presence of the four electronegative adjacent heteroatoms, which cause the C_{ipso}-C_{bridge} bonds to shrink due to their electron withdrawing ability.

In comparison to compounds **2 – 4** the observed C_{ipso}-C_{bridge} distances (1.384 Å to 1.390 Å) are half way between a typical C(sp^2)-C(sp^2) single bond (1.47 Å) and a C(sp^2)=C(sp^2) double bond (1.34 Å), which is a result of the efficient delocalisation of the double bonds. The same explanation is valid for the C_{ipso}-N bond lengths, which are in a narrow range from 1.337 Å to 1.351 Å. These values for the C_{ipso}-N bond lengths can also be seen as the average of a typical C(sp^2)-N(sp^2) single bond (1.40 Å) and a C(sp^2)=N(sp^2) double bond (1.29 Å).[23] In the light of previous results of the methanides $[Me_2Al\{(NCOC_6H_4)_2CH\}]$ and $[Me_2Al\{(NCSC_6H_4)_2CH\}]$[18] and the analogue amide bridged species $[Me_2Al\{(NCSC_6H_4)_2N\}]$ and $[Me_2Al\{(4\text{-}MeNCSC_6H_4)_2N\}]$[19] the discussed structural values are matching well (Table 1).

Table 1. Selected averaged bond lengths (Å) and angles (deg) of the ligand backbone for compounds **1 – 4** and reference structures.

	C_{ipso}–C1'	C_{ipso}–N	C1–C1'–C8
$(4\text{-}MeNCOC_6H_4)_2CH_2$ (**1**)	1.487(2)	1.291(2)	110.79(12)
$[Me_2Al\{(4\text{-}MeNCOC_6H_4)_2CH\}]$ (**2**)	1.384(2)	1.351(2)	121.13(14)
$[Me_2Ga\{(4\text{-}MeNCOC_6H_4)_2CH\}]$ (**3**)	1.388(3)	1.341(2)	121.62(18)
$[Me_2In\{(4\text{-}MeNCOC_6H_4)_2CH\}]$ (**4**)	1.390(13)	1.337(12)	123.6(6)
$[Me_2Al\{(NCOC_6H_4)_2CH\}]$[18]	1.380(3)	1.346(3)	119.5(2)
$[Me_2Al\{(NCSC_6H_4)_2CH\}]$[18]	1.390(2)	1.352(2)	123.54(14)
$[Me_2Al\{(NCSC_6H_4)_2N\}]$[19]	-	1.331(3)	-
$[Me_2Al\{(4\text{-}MeNCSC_6H_4)_2N\}]$[19]	-	1.343(2)	-

Compounds **2** and **3** are equi-structural and crystallise each in the monoclinic space group $P2_1/c$ and the asymmetric unit contains one molecule. **4** crystallises in the monoclinic space group *Pn* and contains two metallated molecules in the asymmetric unit.

The structural comparison of the MMe_2 derivatives shows that in each case the metal coordination again is accomplished by the two nitrogen atoms of the benzoxazole moieties and the oxygen atoms are pointing away from the metal. In all three cases this leads to a distorted tetrahedral coordination geometry at the particular metal ion. As expected the ligand framework in **2 – 4** exhibits nearly no folding of the heterocyclic residues. Additionally the metal ion is located in the C_3N_2 plane of the central six-membered metalla

heterocycle without any significant deviation (see Table 2). Only this arrangement facilitates total conjugation of the whole anionic ligand. Due to the fourfold coordination of the metal ion the methyl residues at that metal are aligned perpendicularly with respect to the N1-M-N2 plane. This V-shaped arrangement of the MMe_2 fragments allows the organometallic fragment to slot in between the methyl groups of the ligand. The four methyl groups frame the group 13 metal to stay in plane (see Figure 6).

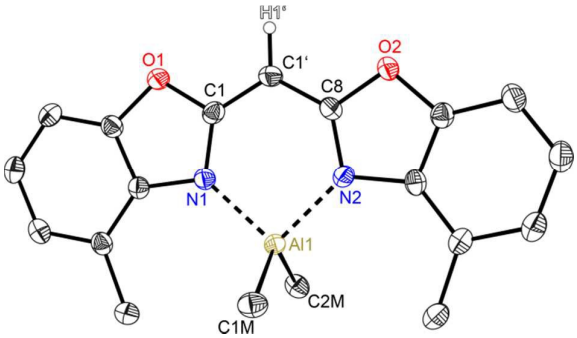

Figure 3. Molecular structure of $[Me_2Al\{(4\text{-Me-}NCOC_6H_3)_2CH\}]$ (**2**). Anisotropic displacement parameters are depicted at the 50 % probability level. C-H hydrogen atoms are omitted for clarity except the one at the bridging CH group. Structural data are given in Tables 1 – 3.

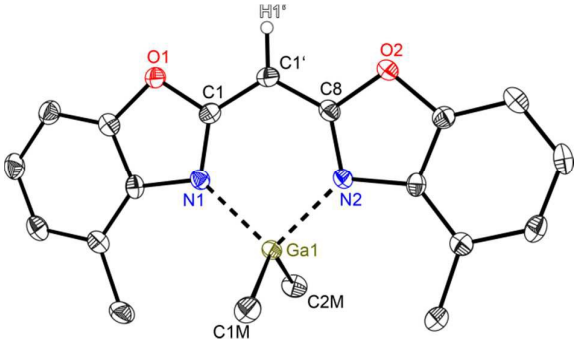

Figure 4. Molecular structure of $[Me_2Ga\{(4\text{-Me-NCO }C_6H_3)_2CH\}]$ (**3**). Anisotropic displacement parameters are depicted at the 50 % probability level. C-H hydrogen atoms are omitted for clarity except the one at the bridging CH group. Structural data are given in Tables 1 – 3.

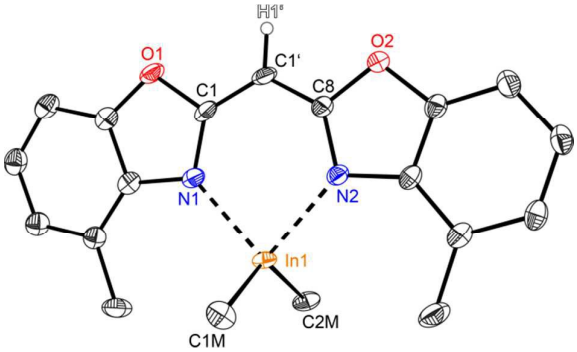

Figure 5. Molecular structure of one molecule of $[Me_2In\{(4\text{-Me-}NCOC_6H_3)_2CH\}]$ (**4**). Anisotropic displacement parameters are depicted at the 50 % probability level. C-H hydrogen atoms are omitted for clarity except the one at the bridging CH group. Structural data are given in Tables 1 – 3.

Table 2. Selected folding parameters for compounds **1** – **7**.

	folding angle [deg]	M-plane distance [Å]
1	-	-
2	3.721(20)	0.0054(22)
3	3.803(20)	0.0068(23)
4*	4.925(122) 6.225(263)	0.0572(287) 0.1545(269)
5	3.394(20)	0.0090(19)
6	3.042(16)	0.0226(37)
7	4.425(71)	0.0483(20)

* two values are given due to the discrepancy of the two molecules within the unit cell.

In the row of the investigated group 13 metal complexes **2** – **4** of the bis-(4-methylbenzoxazol-2-yl)-methanide ligand some clear trends from the obtained structural data could be deduced (see Table 3):

- The transannular N1···N2 distance, which is indicative for the size of the chelated metal atom, increases from **2** over **3** to **4** as expected, because the bigger the coordinated ion is, the wider the chelating distance has to open.
- Also the observed N-M distances are increasing according to the increasing ionic radii of the Al^{3+}, Ga^{3+} or In^{3+} ion, respectively.
- As a further consequence of this bond elongation and due to the fact, that the metal stays in the ligand plane the resulting N1-M-N2 bite angles are decreasing from **2** over **3** to **4**.

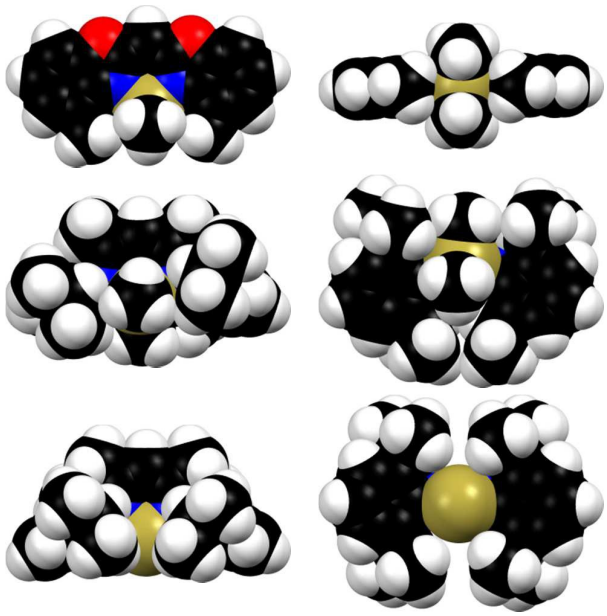

Figure 6. Space filling models from different perspectives (*left column*: front view, *right column*: bottom view) of the compared aluminium complexes **2** (*top*), $[Me_2Al\{Dipp_2\text{-nacnac}\}]$[13i] (**A**) (*middle*) and $[Al\{Dipp_2nacnac\}]$[14e] (**B**) (*bottom*).

In Figure 6 compound **2** is exemplarily compared to the literature known nacnac derivatives $[Me_2Al\{Dipp_2nacnac\}]$[13i] (**A**) and $[Al\{Dipp_2nacnac\}]$[14e] (**B**) containing also the Al(III)Me_2 or Al(I) moiety, respectively. From the space filling model the steric demand of each ligand can be visualised and provides a fair estimate of the shielding abilities around the metal atoms.

Table 3. Selected averaged bond lengths (Å) and angles (deg) for compounds **1 – 7**.

	N1···N2	N1/2–M	C15/16···M	N1–M–N2
1	3.5448(18)	-	-	-
2	2.8534(19)	1.9400(14)	3.4478(19)	94.68(6)
3	2.9010(23)	2.0043(15)	3.4474(22)	92.73(6)
4	3.0485(55)	2.217(9)	3.4805(167)	86.89(14)
5	2.8500(20)	1.9097(14)	3.4736(19)	96.52(6)
6	2.8775(37)	1.909(2)	3.5380(25)	97.84(12)
7	2.8753(21)	1.9140(16)	3.5341(22)	97.38(7)
A	2.870(4)	1.929(2)	3.789(3)	96.18(9)
B	2.764(3)	1.958(2)	3.606(3)	89.86(8)

Starting with the crystal structure of the Al(I) species **B** it is evident, that the metal atom is located almost ideally within the chelating C_3N_2 plane (Figure 6, *bottom*). The N,N'-coordinated metal atom fits well into the pocket made up from the four *i*Pr groups of the Dipp substituents and the carbon atoms in ortho-position of the associated phenyl rings. Furthermore, these phenyl rings are nearly perpendicularly aligned with respect to the C_3N_2 plane (89 ° and 91 °). The ortho-carbon atoms provide the closest contact to the aluminium atom (averaged 3.606 Å) and presumably are equally important for the shielding of low-valent Al(I) species (listed in column C15/16···M in Table 3), because these distances are located between the nacnac species and the complexes derived from **1**. The bottom view also shows that the aluminium atom is not exhaustively coordinated so that coordination of the Lewis acidic site is facilitated. The side view highlights the good shielding abilities of the *i*Pr groups, preventing the molecule from aggregation.

Continuing with the dimethyl aluminium species **A** the crystal structure clearly deviates from the reduced species **B**. The central six-membered metalla heterocycle is less planar than in **B**, because the $AlMe_2$ unit is not located in the chelating C_3N_2 plane. Furthermore, one of the two phenyl rings of the Dipp-substituents is considerably twisted away from orthogonality with respect to the C_3N_2 plane (112 °). This deviation is caused by the additional methyl groups at the aluminium, which increases the steric demand compared to the naked metal in **B**. The formed pocket in **B** is not appropriate in size to accommodate the additional methyl groups. Instead of retaining the perpendicular alignment of the Dipp-substituents one of them is pushed away.

As mentioned earlier the methyl substituents of the chelating ligand in **2** adopt the shielding role of the Dipp residues of the comparable nacnac complexes. This efficient shielding abilities are visualised in the space filling model at the bottom view of **2** in Figure 6: by chelation of the two nitrogen donor atoms of the ligand the $AlMe_2$ fragment is aligned in the C_3N_2 plane without any significant deviation. This planarity is also supported by the ligand's methyl groups, which fit nearly perfectly in between the pocket made up by the V-shaped coordinated $AlMe_2$ cation. So in comparison to **A** and **B** the kinetic shielding considered from the bottom view is even more pronounced. As opposed to this the side view of **2** shows that the planar arrangement of the complex leads to less steric congestion from this point of view. The shielding abilities in **2** are not that embracing like in the case of **A** and **B**, so that still beneficial, specific substitution reactions at the metal centre can take place. This advantageous property is exploited by the synthesis of **5** described in the following paragraph.

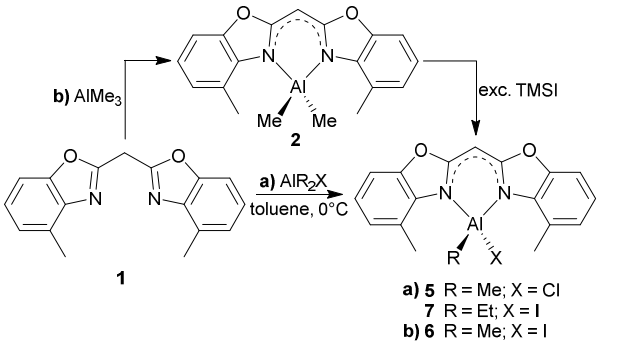

Scheme 3: Synthesis route for the mono halide substituted aluminium complexes **5 – 7**.

Structural comparison of 5 – 7:

In addition to the dimethyl substituted group 13 metal complexes **2 – 4** three Al(III) derivatives, in which one of the methyl groups is replaced by a halide, were successfully synthesised as well. This substitution is necessary to improve the reactivity of those species compared to the relative high stability of the dimethyl aluminium complexes. These reaction products should facilitate the access to Al(I) or Al(II) species upon reductive dehalogenation reactions.

The synthesis of compounds **5** and **7** parallels the procedures to the abovementioned dimethyl derivatives. To a solution of the parent ligand **1** in toluene the pure organometallic reagent $AlMe_2Cl$ or $AlEt_2I$, respectively, was added in a slight excess at 0 °C (Scheme 3, pathway a). Differently **6** was prepared starting from the metallated species **2** by reaction with an excess of trimethyl silyl iododide to prompt a methyl iodide exchange at the metal atom (Scheme 3, pathway b).

Having a closer look at the geometrical data of those halide substituted species **5 – 7** following conclusions can be made: The derivatives **5** (Figure 7) and **7** (Figure 9) crystallise in the monoclinic space group $P2_1/c$ each and the asymmetric unit consists in both cases of one target molecule. Compound **6** (Figure 8) crystallises in the orthorhombic space group *Pbcm* and the asymmetric unit contains half a molecule.

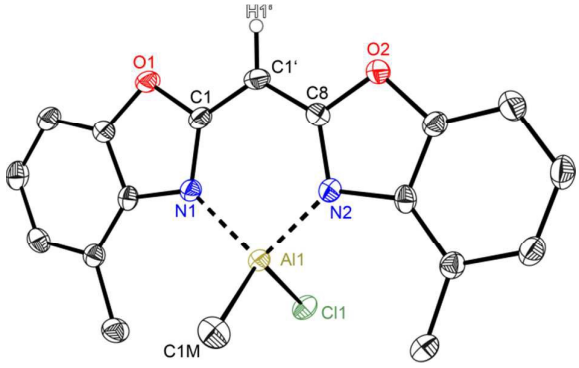

Figure 7. Molecular structure of [ClMeAl{(4-Me-NCOC$_6$H$_3$)$_2$ CH}] (**5**). Anisotropic displacement parameters are depicted at the 50 % probability level. C-H hydrogen atoms are omitted for clarity except the one at the bridging CH group. Structural data are given in Tables 1 – 3.

In the halogenated complexes the aluminium atom adopts also the distorted tetrahedral coordination by means of the two nitrogen donors and the remaining substituents at the metal atom. In direct comparison to the AlMe$_2$ derivative **2** the N-Al distances in **5** – **7** are increased and consequentially the corresponding N-Al-N bite angle is widened (see Table 3). Those observed changes are caused by the electron withdrawing halide ligands Cl or I. These substituents increase the partial positive charge at the metal atom due to the negative inductive effect and their reduced electronegativity compared to carbon. The substituted aluminium atom needs less electron density from the donating nitrogen ring atoms and the nitrogen Lewis donors are less attractive.

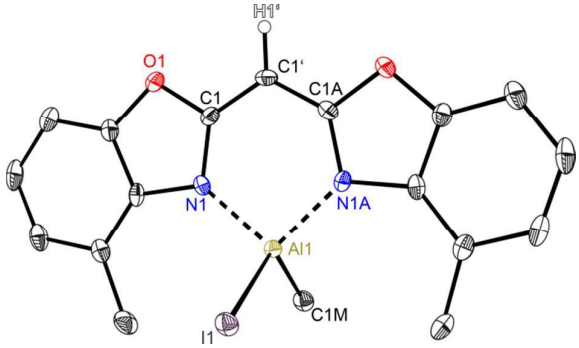

Figure 8. Molecular structure of [IMeAl{(4-Me-NCOC$_6$H$_3$)$_2$ CH}] (**6**). Anisotropic displacement parameters are depicted at the 50 % probability level. C-H hydrogen atoms are omitted for clarity except the one at the bridging CH group. Structural data are given in Tables 1 – 3.

The influence of the present halide atom on specific binding properties is displayed in Table 3. **5** compared to **6** shows the bigger halide iodide to cause the transannular N1···N2 distance to increase by about 0.03 Å (2.8500 Å in **5** vs. 2.8775 Å in **6**). This widening of the coordination pocket is also displayed in the bite angle, which also gets enlarged from 96.52 ° to 97.84 °. Predominantly the higher steric demand of the iodide compared to the chloride accounts for the structural changes in the ligand. The observed differences among the two iodide derivatives **6** and **7** concerning those values are negligible. Within the triple estimated standard deviations the values for both species are the same, indicating that the slightly enhanced steric demand in **7** due to the ethyl group instead of a methyl group has no significant effect on those structural features.

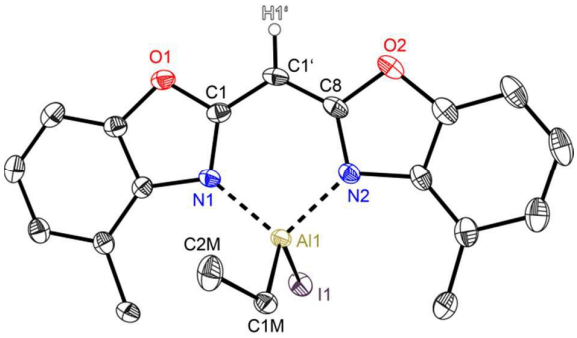

Figure 9. Molecular structure of [IEtAl{(4-Me-NCOC$_6$H$_3$)$_2$ CH}] (**7**). Anisotropic displacement parameters are depicted at the 50 % probability level. C-H hydrogen atoms are omitted for clarity except the one at the bridging CH group. Structural data are given in Tables 1 – 3.

Conclusions

Within this work the successful syntheses and solid state structure determinations of six metallated bis-(4-methylbenz-oxazol-2-yl)-methanides **2** – **7** and the parent uncharged methane derivative **1** could be presented. As a consequence of tuning the previously reported bisheterocyclo methanes by introducing methyl groups to the benzannulated heterocycles (in this case benzoxazole) a promising ligand system for metal complexation could be obtained, which exhibits a nearly perfect planar coordination geometry concerning the ligand side arms in all discussed solid state structures. This fact is displayed by the small values in the folding angles between both heteroaromatic planes and the just slight deviations of the metal cations from the chelating C_3N_2 plane in each complex, which is outstanding in the row of the previously investigated methanide and amide complexes. The observed arrangement in the solid state can be explained by the steric strain induced by the additional methyl groups, which fit inside the properly shaped pocket made up from the particular V-shaped MR$_2$ fragments, so that a kind of intramolecular interlocking is responsible for the overall planar arrangement.
Due to the relatively pronounced inertness of the dimethyl group 13 metal complexes the switch to the mono halide substituted compounds **5** – **7** offers the access to low-valent group 13 complexes, which hopefully can be obtained by reductive salt elimination analogue to the synthesis route of [Al{Dipp$_2$nacnac}] or [Ga{Dipp$_2$nacnac}]. The steric protection around the metal centre resulting from the planar organic ligand is quite efficient for kinetic stabilisation, but in the case of **2** the reaction with an excess of trimethyl silyl iodide showed, that specific substitution reactions can still take place, which is beneficial in contrast to the former nacnac derivatives. Nevertheless, it is worth to mention, that even an excess of TMSI does not lead to a dual halide substituted

derivative. Because of the beneficial planar arrangement of the ligand system and the metal cation within the precursors **2**, **5** – **7** the generation of new Al(I) species is feasible. The planar coordination geometry should enable optimal orbital overlapping between the endocyclic nitrogen donors and the chelated future low-valent metal atom to obtain a more efficient delocalisation. Further substitution and reduction attempts on aluminium containing complexes of this promising ligand system are under investigation.

Experimental Section

General Procedures:

All manipulations were carried out under an atmosphere of dried and purified N_2 or Ar by using Schlenk techniques.[24] All solvents used within metallation reactions were distilled from Na or K prior to use. The starting materials were purchased commercially and used as received. ^{1}H, ^{13}C, ^{15}N and ^{27}Al NMR spectroscopic data were recorded on a Bruker Avance 500 MHz, Bruker Avance 400 MHz and a Bruker Avance 300 MHz spectrometer and referenced to the deuterated solvent (thf-d_8).[25] Elemental analyses (C, H, N and S) were carried out on a Vario EL3 at the Mikroanalytisches Labor, Institut für Anorganische Chemie, University of Göttingen. All EI-MS spectra (70 eV) were recorded on a Finnigan MAT 95.

(4-Me-NCOC$_6$H$_3$)$_2$CH$_2$ (1):

Method 1: 2-Amino-3-methylphenol (2.91 g, 23.6 mmol, 2.00 eq.) and ethylbisimidate dihydrochloride (2.73 g, 11.8 mmol, 1.00 eq.) were dissolved in methanol (55 mL). The heating time of the reaction mixture was extended for reflux overnight and after cooling to rt stored at −32 °C in a refrigerator. The resulting crystalline material was filtered off, washed with saturated aqueous $NaHCO_3$ solution (3 x 50 mL) and water (3 x 50 mL) and dried under reduced pressure. Crystals suitable for X-ray diffraction experiments could be obtained upon recrystallisation from toluene. Pale brown crystals were obtained in a yield of 1.43 g (5.15 mmol, 44 %).

Method 2: A mixture of 2-amino-3-methylphenol (9.85 g, 80.0 mmol, 2.00 eq.) and malonic acid (4.16 g, 40.0 mmol, 1.00 eq.) was suspended in polyphosphoric acid (100 mL) with the use of a sealed precision glass (KPG) stirrer. Under vigorous stirring the reaction mixture was heated to 150 °C and the resulting dark blue viscous solution was kept stirring at this elevated temperature for 5 h. Then the solution was allowed to cool to about 90 °C and poured over ice. The formed grey solid was filtered off, washed several times with saturated aqueous $NaHCO_3$ solution (9 x 50 mL) and distilled water (10 x 50 mL) to pH neutrality. Remaining solvent was evaporated in vacuo to obtain **1** (6.26 g, 22.5 mmol, 56 %) as pale grey powder.

Anal. Calcd. for $C_{17}H_{14}N_2O_2$ (278.31 g/mol): C, 73.37; H, 5.07; N, 10.07. Found: C, 72.90; H, 5.14; N, 9.90; δ^1H (300 MHz, thf-d_8): 7.33 (d, $^3J_{HH}$ = 8.1 Hz, 2 H, H3), 7.20 (t, $^3J_{HH}$ = 7.8 Hz, 2 H, H4), 7.11 (d, $^3J_{HH}$ = 7.5 Hz, 2 H, H5), 4.68 (s, 2 H, H1'), 2.55 (s, 6 H, H15); δ^{13}C{^{1}H} (75 MHz, thf-d_8): 160.62 (s, 2 C, C1), 152.05 (s, 2 C, C2), 141.74 (s, 2 C, C7), 131.32 (s, 2 C, C6), 125.62 (s, 2 C, C4), 125.58 (s, 2 C, C5), 108.58 (s, 2 C, C3), 29.69 (s, 1 C, C1'), 16.41 (s, 2 C, C15); δ^{15}N{^{1}H} (30 MHz, thf-d_8): −135.9 (s); EI-MS, *m/z* (%): 278 (100) $[M]^+$, 146 (10) $[M - NCOC_7H_6]^+$.

Metallation reactions:

To a solution of the corresponding ligand **1** (1.00 eq.) in toluene a slight excess of the pure organometallic reactant $AlMe_3$, $GaMe_3$, $InMe_3$, $AlMe_2Cl$ or $AlEt_2I$, respectively, (1.10 eq.) was slowly added at 0 °C. The reaction mixture was stirred overnight and allowed to warm to rt. Afterwards the volume of the solution was reduced to a few mL and the resulting concentrated solution stored at −32 °C in a refrigerator. Overnight crystals suitable for X-ray diffraction experiments could be obtained. The crystals thus formed were filtered, washed twice with pre-cooled toluene or hexane (0 °C) and finally dried in vacuum. The given yields below are just based on the received crystals unless stated otherwise. No further improvement of the yields was attempted.

[Me$_2$Al{(4-Me-NCOC$_6$H$_3$)$_2$CH}] (2): 1 (4.66 g, 16.7 mmol, 1.00 eq.) dissolved in toluene (120 mL) and trimethyl aluminium (1.80 mL, 1.33 g, 18.4 mmol, 1.10 eq.) were treated like stated in the general procedure above. Yellow crystals were obtained in a yield of 3.79 g (11.3 mmol, 68 %). Anal. Calcd. for $C_{19}H_{19}AlN_2O_2$ (334.35 g/mol): C, 68.25; H, 5.73; N, 8.38. Found: C, 68.21; H, 6.18; N, 8.30; δ^1H (500 MHz, thf-d_8): 7.26 – 7.22 (m, 2 H, H3), 7.11 – 7.06 (m, 4 H, H4 + H5), 5.33 (s, 1 H, H1'), 2.66 (s, 6 H, H15), −0.38 (s, 6 H, H1M); δ^{13}C{^{1}H} (125 MHz, thf-d_8): 168.70 (s, 2 C, C1), 149.29 (s, 2 C, C2), 136.98 (s, 2 C, C7), 127.63 (s, 2 C, C5), 124.33 (s, 2 C, C6), 123.81 (s, 2 C, C4), 108.01 (s, 2 C, C3), 59.95 (s, 1 C, C1'), 19.51 (s, 2 C, C15), −3.86 (s, 2 C, C1M); δ^{15}N{^{1}H} (50 MHz, thf-d_8): −230.5 (s); δ^{27}Al{^{1}H} (130 MHz, thf-d_8): 153 (s); EI-MS, *m/z* (%): 334.1 (10) $[M]^+$, 319.1 (64) $[M - Me]^+$, 303.1 (5) $[M - 2\,Me]^+$, 278.1 (100) $[M - AlMe_2]^+$.

[Me$_2$Ga{(4-Me-NCOC$_6$H$_3$)$_2$CH}] (3): 1 (1.39 g, 5.00 mmol, 1.00 eq.) dissolved in toluene (25 mL) and trimethyl gallium (0.56 mL, 632 mg, 5.50 mmol, 1.10 eq.) were treated like stated in the general procedure above. Brownish yellow crystals were obtained in a yield of 308 mg (0.82 mmol, 17 %; not optimised). Anal. Calcd. for $C_{19}H_{19}GaN_2O_2$ (377.10 g/mol): C, 60.52; H, 5.08; N, 7.43. Found: C, 60.84; H, 5.24; N, 7.45; δ^1H (400 MHz, thf-d_8): 7.22 – 7.13 (m, 2 H, H3), 7.07 – 6.99 (m, 4 H, H4 + H5), 5.18 (s, 1 H, H1'), 2.57 (s, 6 H, H15), 0.06 (s, 6 H, H1M); δ^{13}C{^{1}H} (75 MHz, thf-d_8): 167.84 (s, 2 C, C1), 149.20 (s, 2 C, C2), 137.57 (s, 2 C, C7), 127.27 (s, 2 C, C5), 123.60 (s, 2 C, C6), 123.15 (s, 2 C, C4), 107.85 (s, 2 C, C3), 58.83 (s, 1 C, C1'), 19.01 (s, 2 C, C15), −0.95 (s, 2 C, C1M); δ^{15}N{^{1}H} (40 MHz, thf-d_8): −229.7 (s); EI-MS, *m/z* (%): 376.1 (17) $[M]^+$, 361.0 (100) $[M - Me]^+$, 346.0 (20) $[M - 2\,Me]^+$, 277.1 (12) $[M - GaMe_2]^+$, 68.9 (41) Ga^+.

[Me$_2$In{(4-Me-NCOC$_6$H$_3$)$_2$CH}] (4): 1 (278 mg, 1.00 mmol, 1.00 eq.) dissolved in toluene (60 mL) and trimethyl indium (0.30 mL) were treated like stated in the general procedure above. Because the used $InMe_3$ solution had an unknown concentration, no further statements regarding the equivalents or yield can be made. Orange crystals were obtained in a yield of 78 mg (0.18 mmol). Anal. Calcd. for

Table 4. Crystal structure data for **1** – **7**.

	1	**2**	**3**	**4**	**5**	**6**	**7**
Formula	$C_{17}H_{14}N_2O_2$	$C_{19}H_{19}AlN_2O_2$	$C_{19}H_{19}GaN_2O_2$	$C_{19}H_{19}InN_2O_2$	$C_{18.1}H_{16.3}AlCl_{0.9}N_2O_2$	$C_{18}H_{16}AlIN_2O_2$	$C_{19}H_{18}AlIN_2O_2$
Mol. w., g mol^{-1}	278.31	334.35	377.10	422.18	352.59	446.21	460.23
CCDC no.	1429338	1429357	1429403	1429339	1429341	1429342	1429343
Wavelength, Å	0.71073	0.71073	0.56086	0.56086	0.56086	0.56086	0.71073
Crystal system	triclinic	monoclinic	monoclinic	monoclinic	monoclinic	orthorhombic	monoclinic
Space group	$P\bar{1}$	$P2_1/c$	$P2_1/c$	Pn	$P2_1/c$	$Pbcm$	$P2_1/c$
a, Å	4.741(2)	8.029(2)	7.986(2)	15.629(3)	7.982(2)	8.015(2)	9.102(3)
b, Å	11.471(3)	14.773(3)	14.852(3)	7.894(2)	14.727(3)	13.868(3)	7.647(2)
c, Å	13.084(3)	14.072(3)	14.087(3)	15.631(3)	13.890(2)	15.566(3)	26.711(4)
α, deg	79.15(2)	90	90	90	90	90	90
β, deg	85.84(2)	90.03(2)	90.12(2)	117.04(2)	91.73(2)	90	96.59(2)
γ, deg	78.19(2)	90	90	90	90	90	90
V, Å^3	683.6(4)	1669.1(6)	1670.81(9)	1717.7(7)	1632.0(6)	1730.2(6)	1846.9(8)
Z	2	4	4	4	4	4	4
Refl. measured	23615	57930	45271	49033	20579	25400	38660
Refl. unique	2495	3060	3069	8534	2904	1915	4398
$R1$ [I>2σ(I)][a]	0.0364	0.0306	0.0248	0.0248	0.0322	0.0222	0.0210
w$R2$ (all refl.)[b]	0.0938	0.0868	0.0672	0.0546	0.0885	0.0542	0.0534
R_{int}	0.0369	0.0384	0.0445	0.0481	0.0370	0.0431	0.0231
Abs. stru. para.[26]	-	-	-	0.11(4)	-	-	-
$\Delta\rho_{fin}$, e Å^{-3}	0.170 / −0.162	0.222 / −0.323	0.386 / −0.372	0.334 / −0.463	0.206 / −0.314	0.502 / −0.894	0.730 / −0.406

a $R1 = \frac{\sum\left\|F_o\right|-\left|F_c\right\|}{\sum\left|F_o\right|}$ b $wR2 = \sqrt{\frac{\sum w(F_o^2-F_c^2)^2}{\sum w(F_o^2)^2}}$; $w = \frac{1}{\sigma^2(F_o^2)+(g_1P)^2+g_2P}$; $P = \frac{(F_o^2+2F_c^2)}{3}$.

$C_{19}H_{19}InN_2O_2$ (422.18 g/mol): C, 54.05; H, 4.54; N, 6.64. Found: C, 54.52; H, 4.92; N, 6.70; δ^1H (500 MHz, thf-d$_8$): 7.18 – 7.13 (m, 2 H, H3), 7.00 – 6.95 (m, 4 H, H4 + H5), 5.12 (s, 1 H, H1'), 2.54 (s, 6 H, H15), 0.13 (s, 6 H, H1M); δ^{13}C{^{1}H} (125 MHz, thf-d$_8$): 168.36 (s, 2 C, C1), 148.95 (s, 2 C, C2), 139.27 (s, 2 C, C7), 126.58 (s, 2 C, C5), 122.94 (s, 2 C, C6), 122.66 (s, 2 C, C4), 107.81 (s, 2 C, C3), 59.07 (s, 1 C, C1'), 18.59 (s, 2 C, C15), −2.91 (s, 2 C, C1M); δ^{15}N{^{1}H} (50 MHz, thf-d$_8$): −226.2 (s).

[ClMeAl{(4-Me-NCOC$_6$H$_3$)$_2$CH}] (5): 1 (1.39 g, 5.00 mmol, 1.00 eq.) dissolved in toluene (35 mL) and dimethyl aluminium chloride (0.51 mL, 509 mg, 5.50 mmol, 1.10 eq.) were treated like stated in the general procedure above. A pale yellow powder was obtained in a yield of 1.37 g (3.9 mmol, 77 %). Anal. Calcd. for $C_{18}H_{16}AlClN_2O_2$ (354.77 g/mol): C, 60.94; H, 4.55; N, 7.90. Found: C, 60.99; H, 4.57; N, 8.17; δ^1H (400 MHz, thf-d$_8$): 7.33 – 7.27 (m, 2 H, H3), 7.17 – 7.11 (m, 4 H, H4 + H5), 5.55 (s, 1 H, H1'), 2.78 (s, 6 H, H15), −0.14 (s, 3 H, H1M); δ^{13}C{^{1}H} (125 MHz, thf-d$_8$): 168.67 (s, 2 C, C1), 149.14 (s, 2 C, C2), 136.07 (s, 2 C, C7), 128.02 (s, 2 C, C5), 125.05 (s, 2 C, C6), 124.54 (s, 2 C, C4), 108.24 (s, 2 C, C3), 61.18 (s, 1 C, C1'), 19.93 (s, 2 C, C15), −3.68 (s, 1 C, C1M); δ^{15}N{^{1}H} (50 MHz, thf-d$_8$): −246.9 (s); δ^{27}Al{^{1}H} (78 MHz, thf-d$_8$): 128 (s); EI-MS, *m/z* (%): 278 (100) [M – AlMeCl]$^+$, 146 (45) [M – AlMeCl – NCOC$_7$H$_6$]$^+$, 132 (8) [NCOC$_7$H$_6$]$^+$.

[IMeAl{(4-Me-NCOC$_6$H$_3$)$_2$CH}] (6): To a solution of **2** (334 mg, 1.00 mmol, 1.00 eq.) in toluene (20 mL) was added trimethylsilyl iodide (0.31 mL, 440 mg, 2.20 mmol, 2.20 eq.). The reaction mixture was heated to reflux temperature and stirred for additional 3.5 d at reflux. The formed precipitate was filtered off and residual solvent was removed under reduced pressure. The mono iodide substituted derivative could be isolated as a brown powder (111 mg, 0.25 mmol, 25 %). After recrystallization from toluene also crystals suitable for structure determination were obtained. Calcd. for $C_{18}H_{16}AlIN_2O_2$ (446.22 g/mol): C, 48.45; H, 3.61; N, 6.28. Found: C, 45.53; H, 3.32; N, 6.07 (deviation due to slight contamination with the AlI$_2$ derivative); δ^1H (300 MHz, thf-d$_8$): 7.29 – 7.25 (m, 2 H, H3), 7.14 – 7.10 (m, 4 H, H4 + H5), 5.47 (s, 1 H, H1'), 2.77 (s, 6 H, H15), −0.47 (s, 3 H, H1M); δ^{13}C{^{1}H} (125 MHz, thf-d$_8$): 168.90 (s, 2 C, C1), 149.13 (s, 2 C, C2), 136.66 (s, 2 C, C7), 127.72 (s, 2 C, C5), 125.12 (s, 2 C, C6), 124.11 (s, 2 C, C4), 108.05 (s, 2 C, C3), 60.58 (s, 1 C, C1'), 18.88 (s, 2 C, C15), −6.83 (s, 1 C, C1M); δ^{15}N{^{1}H} (50 MHz, thf-d$_8$): −230.8 (s); EI-MS, *m/z* (%): 278 (100) [M – AlMeI]$^+$, 146 (37) [M – AlMeI – NCOC$_7$H$_6$]$^+$, 132 (9) [NCOC$_7$H$_6$]$^+$.

[IEtAl{(4-Me-NCOC$_6$H$_3$)$_2$CH}] (7): To a solution of **1** (1.39 g, 5.00 mmol, 1.00 eq.) dissolved in toluene (80 mL) and diethylaluminium iodide (0.73 mL, 1.17 g, 5.50 mmol, 1.10 eq.) were treated like stated in the general procedure above. Orange crystals were obtained in a yield of 1.16 g (2.52 mmol, 50 %; not optimised). Calcd. for $C_{19}H_{18}AlIN_2O_2$ (460.24 g/mol): C, 49.58; H, 3.94; N, 6.09. Found: C, 49.35; H, 4.02; N, 6.09; δ^1H (400 MHz, thf-d$_8$): 7.29 – 7.24 (m, 2 H, H3), 7.14 – 7.11 (m, 4 H, H4 + H5), 5.46 (s, 1 H, H1'), 2.79 (s, 6 H, H15), 0.85 (t, $^3J_{HH}$ = 8.2 Hz, 3 H, H2M), 0.21 (q, $^3J_{HH}$ = 8.2 Hz, 2 H, H1M); δ^{13}C{^{1}H} (75 MHz, thf-d$_8$): 169.09 (s, 2 C, C1), 149.12 (s, 2 C, C2), 136.72 (s, 2 C, C7), 127.73 (s, 2 C, C5), 125.15 (s, 2 C, C6), 124.10 (s, 2 C, C4), 108.05 (s, 2 C, C3), 60.52 (s, 1 C, C1'), 18.74 (s, 2 C, C15), 8.66 (s, 1 C, C2M), 3.13 (s, 1 C, C1M); δ^{15}N{^{1}H} (40 MHz, thf-d$_8$): −232.3 (s); EI-MS, *m/z* (%): 278 (100)

$[M - AlEtI]^+$, 146 (41) $[M - AlEtI - NCOC_7H_6]^+$, 132 (7) $[NCOC_7H_6]^+$.

X-ray Crystallographic Studies

Single crystals were selected from a Schlenk flask under argon or nitrogen atmosphere and covered with perfluorinated polyether oil on a microscope slide, which was cooled with a nitrogen gas flow using the X-TEMP2 device.[27] An appropriate crystal was selected using a polarise microscope, mounted on the tip of a MiTeGen©MicroMount or glass fibre, fixed to a goniometer head and shock cooled by the crystal cooling device. The data for **1**–**7** were collected from shock-cooled crystals at 100(2) K. The data of **1**, **2** and **7** were collected on an Incoatec Mo Microsource[28] and compounds **3**–**6** were collected on an Incoatec Ag Microsource,[29] each equipped with mirror optics and APEX II detector with a D8 goniometer. All diffractometers were equipped with a low-temperature device and used either MoK_α radiation of $\lambda = 0.71073$ Å or AgK_α radiation of $\lambda = 0.56086$ Å. The data were integrated with Saint[30] and an semi-empirical absorption correction (Sadabs)[29] was applied. The structures were solved by direct methods (Shelxt)[31] and refined by full-matrix least-squares methods against F^2 (Shelxl2014).[32] All non-hydrogen-atoms were refined with anisotropic displacement parameters. The hydrogen atoms were refined isotropically on calculated positions using a riding model with their U_{iso} values constrained to equal to 1.5 times the U_{eq} of their pivot atoms for terminal sp^3 carbon atoms and 1.2 times for all other carbon atoms. Disordered moieties were refined using bond lengths restraints and isotropic displacement parameter restraints. The positions of the amine hydrogen atoms are taken from the difference Fourier map and refined freely.

Crystallographic data for the structures reported in this paper have been deposited with the Cambridge Crystallographic Data Centre. The CCDC numbers, crystal data and experimental details for the X-ray measurements are listed in the ESI. Copies of the data can be obtained free of charge from The Cambridge Crystallographic Data Centre via www.ccdc.cam.ac.uk/data_request/cif or from the corresponding author.

Acknowledgements

Thanks to the Danish National Research Foundation (DNRF93) funded *Center for Materials Crystallography* (CMC) for partial support and the Land Niedersachsen for providing a fellowship in the GAUSS PhD program.

Notes and references

The authors declare no competing financial interest.

1. P. P. Power, *Nature*, 2010, **463**, 171-177.
2. a) D. W. Stephan, *Organic & Biomolecular Chemistry*, 2008, **6**, 1535-1539; b) W. Tochtermann, *Angew. Chem.*, 1966, **7**, 355-375.; *Angew. Chem. Int. Ed. Engl.*, 1966, **5**, 351-371; c) G. Wittig and E. Benz, *Chem. Ber.*, 1959, **92**, 1999-2013.
3. a) D. W. Stephan and G. Erker, *Angew. Chem.*, 2010, **122**, 50-81; *Angew. Chem. Int. Ed.*, 2010, **49**, 46-76; b) P. Spies, G. Kehr, K. Bergander, B. Wibbeling, R. Fröhlich and G. Erker, *Dalton Trans.*, 2009, 1534-1541; c) G. C. Welch, R. R. S. Juan, J. D. Masuda and D. W. Stephan, *Science*, 2006, **314**, 1124-1126.
4. G. C. Welch, J. D. Masuda and D. W. Stephan, *Inorg. Chem.*, 2006, **45**, 478-480.
5. C. Appelt, J. C. Slootweg, K. Lammertsma and W. Uhl, *Angew. Chem.*, 2013, **52**, 4256-4259; *Angew. Chem. Int. Ed.*, 2013, **52**, 4256-4259.
6. Y. Zhang, G. M. Miyake and E. Y. X. Chen, *Angew. Chem.*, 2010, **122**, 10356-10360; *Angew. Chem. Int. Ed.*, 2010, **49**, 10158-10162.
7. a) G. Ménard and D. W. Stephan, *Angew. Chem.*, 2011, **123**, 8546-8549; *Angew. Chem. Int. Ed.*, 2011, **50**, 8396-8399; b) G. Ménard and D. W. Stephan, *J. Am. Chem. Soc.*, 2010, **132**, 1796-1797.
8. L. Bourget-Merle, M. F. Lappert and J. R. Severn, *Chem. Rev.*, 2002, **102**, 3031-3065.
9. a) J. Overgaard, C. Jones, A. Stasch and B. B. Iversen, *J. Am. Chem. Soc.*, 2009, **131**, 4208-4209; b) M. Westerhausen, *Angew. Chem.*, 2008, **120**, 2215-2217; *Angew. Chem. Int. Ed.*, 2008, **47**, 2185-2187; c) S. P. Green, C. Jones and A. Stasch, *Science*, 2007, **318**, 1754-1757.
10. a) C. Ruspic and S. Harder, *Inorg. Chem.*, 2007, **46**, 10426-10433; b) S. Harder, *Organometallics*, 2002, **21**, 3782-3787.
11. D. F. J. Piesik, S. Range and S. Harder, *Organometallics*, 2008, **27**, 6178-6187.
12. J. Spielmann, F. Buch and S. Harder, *Angew. Chem.*, 2008, **120**, 9576-9580; *Angew. Chem. Int. Ed.*, 2008, **47**, 9434-9438.
13. a) Y. Cheng, D. J. Doyle, P. B. Hitchcock and M. F. Lappert, *Dalton Trans.*, 2006, 4449-4460; b) S. Singh, H.-J. Ahn, A. Stasch, V. Jancik, H. W. Roesky, A. Pal, M. Biadene, R. Herbst-Irmer, M. Noltemeyer and H.-G. Schmidt, *Inorg. Chem.*, 2006, **45**, 1853-1860; c) Z. Yang, H. Zhu, X. Ma, J. Chai, H. W. Roesky, C. He, J. Magull, H.-G. Schmidt and M. Noltemeyer, *Inorg. Chem.*, 2006, **45**, 1823-1827; d) N. Kuhn, S. Fuchs and M. Steimann, *Z. Anorg. Allg. Chem.*, 2002, **628**, 458-462; e) N. Kuhn, S. Fuchs and M. Steimann, *Eur. J. Inorg. Chem.*, 2001, **2001**, 359-361; f) M. Stender, B. E. Eichler, N. J. Hardman, P. P. Power, J. Prust, M. Noltemeyer and H. W. Roesky, *Inorg. Chem.*, 2001, **40**, 2794-2799; g) N. Kuhn, J. Fahl, S. Fuchs, M. Steimann, G. Henkel and A. H. Maulitz, *Z. Anorg. Allg. Chem.*, 1999, **625**, 2108-2114; h) C. E. Radzewich, I. A. Guzei and R. F. Jordan, *J. Am. Chem. Soc.*, 1999, **121**, 8673-8674; i) B. Qian, D. L. Ward and M. R. Smith, *Organometallics*, 1998, **17**, 3070-3076.
14. a) S. Nagendran and H. W. Roesky, *Organometallics*, 2008, **27**, 457-492; b) X. Li, X. Cheng, H. Song and C. Cui, *Organometallics*, 2007, **26**, 1039-1043; c) H. W. Roesky and S. S. Kumar, *Chem. Commun.*, 2005, 4027-4038; d) M. N. Sudheendra Rao, H. W. Roesky and G. Anantharaman, *J. Organomet. Chem.*, 2002, **646**, 4-14; e) C. Cui, H. W. Roesky, H.-G. Schmidt, M. Noltemeyer, H. Hao and F. Cimpoesu, *Angew. Chem.*, 2000, **112**, 4444-4446; *Angew. Chem. Int. Ed.*, 2000, **39**, 4274-4276.
15. N. J. Hardman, B. E. Eichler and P. P. Power, *Chem. Commun.*, 2000, 1991-1992.
16. a) P. Hao, Z. Yang, W. Li, X. Ma, H. W. Roesky, Y. Yang and J. Li, *Organometallics*, 2015, **34**, 105-108; b) B. Li, C. Zhang, Y. Yang, H. Zhu and H. W. Roesky, *Inorg. Chem.*, 2015, **54**, 6641-6646; c) Z. Yang, M. Zhong, X. Ma, S. De, C. Anusha, P. Parameswaran and H. W. Roesky, *Angew. Chem.*, 2015, **127**, 10363-10367.; *Angew. Chem. Int. Ed.*, 2015, **54**, 10225-10229; d) Y. Yang, H. Li, C. Wang and H. W. Roesky, *Inorg. Chem.*, 2012, **51**, 2204-2211.

17. a) Z. Zhu, X. Wang, Y. Peng, H. Lei, J. C. Fettinger, E. Rivard and P. P. Power, *Angew. Chem.*, 2009, **121**, 2065-2068; *Angew. Chem. Int. Ed.*, 2009, **48**, 2031-2034; b) R. J. Wright, M. Brynda and P. P. Power, *Angew. Chem.*, 2006, **118**, 6099-6102; *Angew. Chem. Int. Ed.*, 2006, **45**, 5953-5956; c) R. J. Wright, A. D. Phillips, S. Hino and P. P. Power, *J. Am. Chem. Soc.*, 2005, **127**, 4794-4799; d) N. J. Hardman, R. J. Wright, A. D. Phillips and P. P. Power, *Angew. Chem.*, 2002, **114**, 2966-2968; *Angew. Chem. Int. Ed.*, 2002, **41**, 2842-2844; e) J. Su, X.-W. Li, R. C. Crittendon and G. H. Robinson, *J. Am. Chem. Soc.*, 1997, **119**, 5471-5472.
18. D.-R. Dauer and D. Stalke, *Dalton Trans.*, 2014, **43**, 14432-14439.
19. D.-R. Dauer, M. Flügge, R. Herbst-Irmer and D. Stalke, *Dalton Trans.*, 2015, **submitted**.
20. a) F. Baier, Z. Fei, H. Gornitzka, A. Murso, S. Neufeld, M. Pfeiffer, I. Rüdenauer, A. Steiner, T. Stey and D. Stalke, *J. Organomet. Chem.*, 2002, **661**, 111-127; b) H. Gornitzka and D. Stalke, *Angew. Chem.*, **1994**, *106*, 695-698; *Angew. Chem. Int. Ed. Engl.*, 1994, **33**, 693-695; c) H. Gornitzka and D. Stalke, *Organometallics*, 1994, **13**, 4398-4405.
21. W. W. Schoeller, *Inorg. Chem.*, 2011, **50**, 2629-2633.
22. H. Ben Ammar, J. Le Nôtre, M. Salem, M. T. Kaddachi and P. H. Dixneuf, *J. Organomet. Chem.*, 2002, **662**, 63-69.
23. a) P. Müller, R. Herbst-Irmer, A. L. Spek, T. R. Schneider and M. R. Sawaya, *Crystal Structure Refinement A Crystallographer's Guide to SHELXL*, Oxford University Press, New York, 2006; b) P. Rademacher, *Strukturen organischer Moleküle*, VCH, Weinheim, 1987.
24. Georg-August-Universität Göttingen, Virtuelles Labor, http://www.stalke.chemie.uni-goettingen.de/virtuelles_labor/advanced/13_de.html.
25. Georg-August-Universität Göttingen, Virtuelles Labor, http://www.stalke.chemie.uni-goettingen.de/virtuelles_labor/nmr/de.html.
26. S. Parsons, H. D. Flack and T. Wagner, *Acta Crystallogr., Sect. B*, 2013, **69**, 249-259.
27. a) D. Stalke, *Chem. Soc. Rev.*, 1998, **27**, 171-178; b) T. Kottke, R. J. Lagow and D. Stalke, *J. Appl. Crystallogr.*, 1996, **29**, 465-468; c) T. Kottke and D. Stalke, *J. Appl. Crystallogr.*, 1993, **26**, 615-619; d) Georg-August-Universität Göttingen, Virtuelles Labor, http://www.stalke.chemie.uni-goettingen.de/virtuelles_labor/special/22_de.html.
28. T. Schulz, K. Meindl, D. Leusser, D. Stern, J. Graf, C. Michaelsen, M. Ruf, G. M. Sheldrick and D. Stalke, *J. Appl. Crystallogr.*, 2009, **42**, 885-891.
29. L. Krause, R. Herbst-Irmer, G. M. Sheldrick and D. Stalke, *J. Appl. Crystallogr.*, 2015, **48**, 3-10.
30. Bruker AXS Inc., in *Bruker Apex CCD, SAINT v8.30C*, ed. Bruker AXS Inst. Inc., WI, USA, Madison, 2013.
31. G. Sheldrick, *Acta Crystallogr., Sect. A*, 2015, **71**, 3-8.
32. a) G. Sheldrick, *Acta Crystallogr., Sect. C*, 2015, **71**, 3-8; b) G. M. Sheldrick, *Acta Crystallogr., Sect. A*, 2014, **70**, C1437; c) G. M. Sheldrick, *Acta Crystallogr., Sect. A*, 2008, **64**, 112-122.

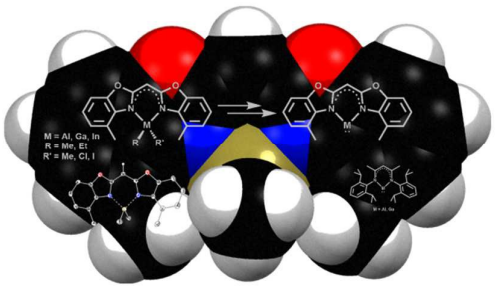

On the basis of the deprotonated bis-(4-methylbenzoxazol-2-yl)-methane ligand **1** a series of group 13 metal complexes was synthesised and fully characterised. The detailed comparison of the solid state structures demonstrates clearly the similarity of the methanide and the omnipresent nacnac ligand, suggesting this ligand system as a promising candidate to stabilise metals in low oxidation states.